

# Vision-Based Grasping and Manipulation of Flexible USB Wires

Yuan Gao, Zhi Chen and Yun-Hui Liu.

*Department of Mechanical and Automation Engineering  
The Chinese University of Hong Kong  
Shatin, NT, Hong Kong  
gaoyuan@link.cuhk.edu.hk*

Mengjun Fang, Jiahuang Lin

*Department of Mechanical Engineering and Automation  
The Harbin Institute of Technology  
Shenzhen, Guangdong Province, China  
fangmengjun@stu.hit.edu.cn*

**Abstract**—The USB wires are commonly used in many 3C products (Computer, Communication and Consumer electronics), such as smartphones, laptops, and tablets. The demand for manufacturing and soldering USB wires is now increasing significantly as the rapidly expanding 3C market. However, because of the small size and the deformation property of USB wires, current soldering procedures are heavily dependent on manual works. There are three steps to solder the USB wires: *Separating, Sorting, and Pressing*. In this paper, it mainly deals with wire sorting and pressing tasks after the wire separation. Vision feedback is applied to the sorting task and it also assesses the status of completion. The developed grasping and manipulation algorithm have the advantage of highly autonomous capability, in sense that no human assistance or supervision is required throughout the procedure. Moreover, it has a certain level of intelligence, the actual operation sequence is not completely fixed, it is based on the principle of the minimum distance between the position of the grasping point and the position of soldering groove, which will improve the overall efficiency.

**Index Terms**—Industrial robot; Vision-based grasping and manipulation; Gripper design; Flexible USB wires

## I. INTRODUCTION

The USB wire is a very common and important accessory for 3C products, for purposes of charging and data transfer. With the rapid expanding of the 3C market, more than billions of USB wires are soldered and manufactured every year [1]. While several machines have been developed to automate one or two steps, a lot of manual works are still required in the procedure of soldering. In particular, humans need to separate the USB wires then manipulating them into the corresponding grooves of the soldering machine (see Fig. 1). The main reason is that the USB wires are highly deformable and need to be dealt with by humans [2].

In the literature, much progress has been achieved in the robotic manipulation of rigid objects [3]–[7]. However, the

research for manipulating the deformable objects is relatively limited. In some industrial and medical scenarios, the manipulation of deformable objects is common. In [8], cable management is proposed in factories. In [9], the organs and tissues are manipulated in medical contexts. In [10]–[12], a model-free method is used to tackle the manipulation of flexible objects. The control algorithm was derived from the on-line deformation model estimation. In [13], [14], a fourier-based shape servo has been proposed, it introduces a vision-feedback characterization of deformable closed shape contours and utilizes it to perform manipulation of soft objects. In [15], a uniform framework that includes state estimation, task planning, and trajectory planning is proposed, which is based on the concept of coherent point drift to knot a soft rope. The path planning method was also employed in [16], [17] to manipulate the deformable linear object to transit from one minimal-energy curve to another, which was represented as the stable configuration. However, a certain level of human assistance or involvement is still required in existing methods for robotic manipulation of deformable objects. For example, humans should initiate or re-establish the physical contact between the robot end-effector and the deformable object in [16], [17], whenever the contact is lost during the manipulation.

This paper considers the problem of robotic grasping and manipulation of USB wires. In the sorting and pressing step, the separated wires are grasped and manipulated to the corresponding soldering groove with the desired USB color code (i.e. RED - WHITE - GREEN - BLACK from left from right). The visual feedback is applied to the sorting and pressing task and it also assesses the status of completion. In some accidental cases, the USB wires will fall off from the soldering groove, which should be avoided in actual production. Therefore, the camera will monitor if the wire grasping and manipulation is successful. The corresponding error correction control strategy is embedded in the sorting and pressing algorithm. Besides, the developed grasping and manipulating platform have the advantage of highly autonomous capability, in sense that no human assistance or supervision is required throughout the procedure. The

Y. Gao, Z. Chen, Y.-H. Liu are with the Department of Mechanical and Automation Engineering, The Chinese University of Hong Kong. M. Fang and J. Lin are with the School of Mechanical Engineering and Automation, The Harbin Institute of Technology. This work was supported in part by the Science and Technology Innovation Council of Shenzhen under Grant no. 20170480, and in part by the Innovation and Technology Commission of Hong Kong under Grant no. ITS/074/17, and in part by the CURI VC's Fund under Grant no.4930745. Corresponding author: Yun-Hui Liu (yhlui@mae.cuhk.edu.hk)

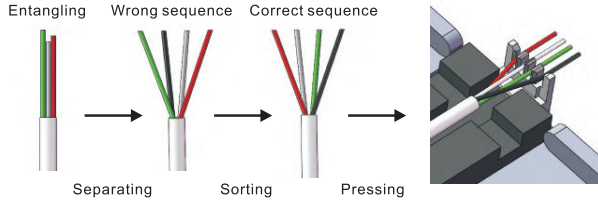


Fig. 1. The pre-processing steps include *Wire Separating*, *Wire Sorting*, and *Wire Pressing*.

experimental results in different scenarios are presented to validate the proposed control strategy.

## II. BACKGROUND

### A. Problem Formulation

The pre-processing of the USB wires in Fig. 1 has been divided into two parts, the first part is *Wire Separating*, and the second part is *Wire Sorting and Pressing*. At first, the four USB wires are separated from each other and then the USB wires will be sorted to follow the desired USB color code (i.e. from left to right, RED - WHITE - GREEN - BLACK) and fixed it into the corresponding grooves. Since the wire separating module in the US patent [18] has already solved the problem of separating the USB wires from the entangling state, this paper mainly deals with *Wire Sorting and Pressing* task after the wire separation. So we assume that all sorting tasks are performed after the wire separation, but the sequence of USB wires is random. Note that the USB color sequence is very important. Otherwise, even the wires are successfully soldered together with the USB head, such wires cannot function properly.

### B. The Overview of Robot Platform

The overall design of the sorting and pressing platform is shown in Fig. 2. which consists of the three modules (i.e. *Grasping Module*, *Aubo Robot Arm*, and *Wire Fixed Module*). The grasping module is specifically designed to grasp and

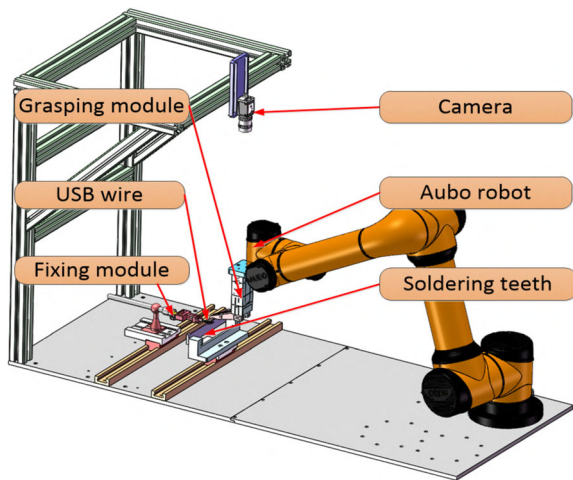


Fig. 2. The overview configuration of the platform.

manipulate the tiny flexible USB wires, which is controlled by a servo motor. The wire fixed module is to fix the root of the USB wires. The robot arm coupled with a 2d camera will do the sorting and pressing task after the image processing.

### C. Robot Kinematics

The Aubo-i5 robot is a 6-DOF collaborative robot. At first, the relationship between the end-effector and the base of the robot needs to be determined. Generally, the coordinate transformation relationship of rigid bodies is obtained by the standard Denavit-Hartenberg method. However, the Standard D-H method may not describe the exact position in Y-axis if there are some assembly errors. Therefore, a modified D-H method in Fig. 3 is adopted and the D-H parameters are list in the Tab. I.

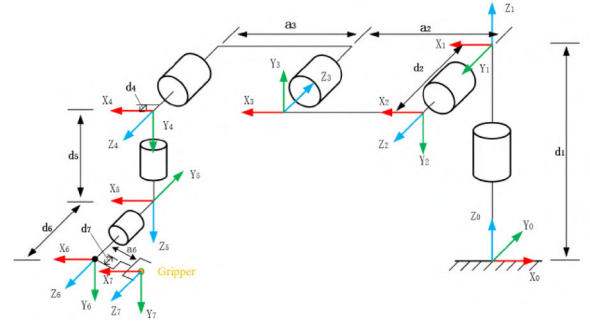


Fig. 3. Link frame assignment of the robot arm.

According to the modified D-H method, the homogeneous transformation matrix between adjacent links is shown in equation 1.

$${}^{i-1}T_i = R_x(\alpha_{i-1})T_x(a_{i-1})R_z(\theta_i)T_z(d_i)$$

$$= \begin{bmatrix} c\theta_i & -s\theta_i & 0 & a_{i-1} \\ s\theta_i c\alpha_{i-1} & c\theta_i c\alpha_{i-1} & -s\alpha_{i-1} & -s\alpha_{i-1}d_i \\ s\theta_i s\alpha_{i-1} & c\theta_i s\alpha_{i-1} & c\alpha_{i-1} & c\alpha_{i-1}d_i \\ 0 & 0 & 0 & 1 \end{bmatrix} \quad (1)$$

After that, the homogeneous transformation matrix of the end effector relative to the robot base can be obtained from equation 2.

$${}^0T_6 = {}^0T_1 {}^1T_2 {}^2T_3 {}^3T_4 {}^4T_5 {}^5T_6 \quad (2)$$

TABLE I  
MODIFIED DENAVIT-HARTENBERG PARAMETERS

ith Joint	$a_{i-1}/m$	$\alpha_{i-1}$	$d_i/m$	$\theta_i$	offset
1	0	0	0.0985	$\theta_1$	0
2	0	$-\pi/2$	0.1405	$\theta_2$	$-\pi/2$
3	0.408	$\pi$	0	$\theta_3$	0
4	0.376	$\pi$	-0.019	$\theta_4$	$-\pi/2$
5	0	$-\pi/2$	0.1025	$\theta_5$	0
6	0	$\pi/2$	0.094	$\theta_6$	0
7	0.085	0	0.115	0	0

In order to grasp and manipulate the USB wires, a small gripper will be mounted on the end of the robot arm. The tool coordinate  $T_{\text{tool}}$  is established in the center of the gripper and the DH parameters are shown in the Tab. I. Finally, the relationship between tool coordinate and the robot base coordinate will be obtained from the kinematic models in equation 3.

$${}^0T_{\text{tool}} = {}^0T_1 T_2 T_3 T_4 T_5 T_6 T_{\text{tool}} \quad (3)$$

### III. ROBOTIC MANIPULATION OF USB WIRES

#### A. Design of Small Gripper

As shown in Fig. 4, the grippers are driven by a servo motor to achieve a stepless adjustment of the spacing  $L$ . During the process of placing the USB wires into the soldering tooth groove, the grippers grasp the wire head to move vertically downward along the tooth groove direction, and the head of the gripper has an U-shaped groove to prevent interference with soldering tooth, the width of the U-shaped groove and the soldering tooth is 1.5mm and 1mm respectively, which can tolerate a certain operational error. The design also ensures that the center of the wire grasping point and the center of the soldering groove are in the same position. The wire head is clamped between the left and right grippers and squeezed into the lower groove. Finally, the grippers open vertically upwards by the direction of the groove.

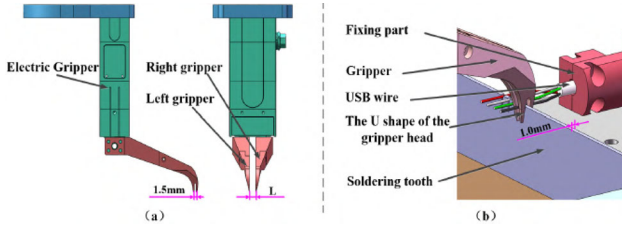


Fig. 4. The structure of the small gripper. (a) The view of gripper component; (b) The view of placing the wire heads into the soldering tooth groove.

#### B. Grasping Point Detection of USB wires

The raw data from the camera is processed by converting the RGB format into the HSV format, such that the processed image is relatively less sensitive to the changes in the illumination, which helps to improve the robustness of the algorithm. Then, the wires with different colors within the known environment can be recognized by setting the parameters of H, S, V. The binary images of the wires are obtained after the color recognition. Then, the snapshots of image processing for obtaining the grasping points are shown in Fig. 5.

- First, the region of interest in the binary image is set.
- Second, the contour of the USB wire is searched and determined.

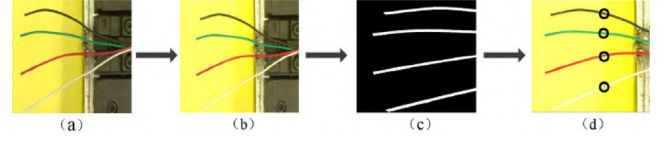


Fig. 5. Snapshots of the image processing: (a) the original image from camera; (b) image enhancement eliminates black shadows; (c) binary effect after color filtering; (d) grasping point from the center moment.

- Third, a minimum bounding rectangle is formulated to enclose the contour.
- Fourth, the center moment  $(i_c, j_c)$  of the rectangular are calculated by using the  $0th$  moment and the  $1st$  moment of the binary image.

The area of the rectangular contour can be calculated from equation 4 and  $V(i, j)$  denote gray value at  $(i, j)$  point.

$$M_{00} = \sum_i \sum_j V(i, j) \quad (4)$$

In equation 5 and equation 6, the first moment in two dimensions of the rectangular contour can be calculated, which are represented by  $M_{10}$  and  $M_{01}$ .

$$M_{10} = \sum_i \sum_j iV(i, j) \quad (5)$$

$$M_{01} = \sum_i \sum_j jV(i, j) \quad (6)$$

- Fifth, the grasping point (center moment) is derived from the equation 7.

$$i_c = \frac{M_{10}}{M_{00}}, j_c = \frac{M_{01}}{M_{00}} \quad (7)$$

#### C. Nine-Point Calibration

The nine-point calibration algorithm is mainly used to obtain the transformation matrix between the pixel coordinate and the robot base coordinate. Generally, the feedback information obtained by the visual sensor is based on the pixel coordinate, and the robot arm cannot directly use the feature information acquired by the camera. In order to enable the robot arm to use the visual feedback after the image processing, the grasping point in the pixel coordinate need to be converted to the robot base coordinate.

Nine-point calibration aims to calculate the affine transformation matrix from the pixel coordinates to the robot base coordinate. In the equation 8, the point  $(u, v, 1)^T$  is the homogeneous coordinate of the image point, and the point  $(x', y', 1')^T$  is the end effector position of robot arm.  $a_{11}, a_{12}, a_{21}, a_{22}$  are elements of the rotation matrix.  $a_{13}, a_{23}$  are the translation matrix. Equation 8 can be further written in the form of Equation 9.

$$\begin{bmatrix} x' \\ y' \\ 1' \end{bmatrix} = \begin{bmatrix} a_{11} & a_{12} & a_{13} \\ a_{21} & a_{22} & a_{23} \\ 0 & 0 & 1 \end{bmatrix} \begin{bmatrix} u \\ v \\ 1 \end{bmatrix} \quad (8)$$

In the equation 9, there are six unknown parameters. All the parameters can be calculated by using 3 sets of corresponding points. Due to the small error of the data point set, 9 sets of points combined with the least-squares are usually used to calculate the affine matrix.

$$\begin{bmatrix} x' \\ y' \\ 1' \end{bmatrix} = \begin{bmatrix} R_{2 \times 2} & T_{2 \times 1} \\ 0_{1 \times 2} & 1 \end{bmatrix} \begin{bmatrix} u \\ v \\ 1 \end{bmatrix} \quad (9)$$

In our platform, the camera is fixedly mounted above the robot arm (eye-to-hand mode) and the transformation matrix  $K$  is as follows,

$$K = \begin{bmatrix} -0.055 & -0.0022 & 160.12 \\ -0.0019 & 0.05414 & -622.6 \\ 0 & 0 & 1 \end{bmatrix} \quad (10)$$

#### D. Control Scheme of USB Wires Sorting

Before sorting, the robot uses a camera to assess the color and the position of four wires. After that, the robot will control the gripper to grasp and manipulate the specific wires. Taking the red wire as an example in Fig. 6. The pixel position of the grasping point is obtained from the image processing. Through the nine-point calibration method introduced in the previous section, the pixel coordinates are transformed into the base coordinate of the robot arm. Through the linear planning control of the robot end-effector, the movement trajectory of the gripper moves from one position to another position in a straight line. The grasping step can be divided into the following 5 steps.

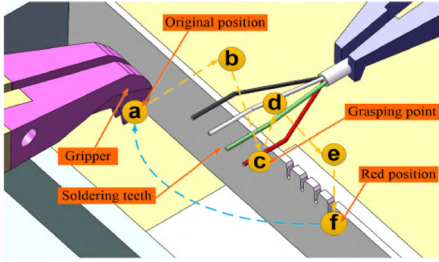


Fig. 6. The grasping schematic of red wire.

- Step 1, the gripper will move from the original position to the upper grasping point of the red wire.
- Step 2, the gripper will control to the preset height to grasp the red wires in the z-direction.
- Step 3, the gripper coupled with red wire will move to a preset height again.
- Step 4, the red wire will be moved on the top of the corresponding soldering groove.
- Step 5, the red wire will be placed into the groove.

In this process, the USB wires are sorted and pressed by the linear planning control of the robot arm. The operation of other USB wires is similar to the above step. Since the

color sequence is random after the wire separation module. To improve the grasping efficiency, the actual operation sequence is not completely fixed, it is based on the principle of the minimum distance between the position of the grasping point and the soldering groove. However, the final desired color sequence must be RED - WHITE - GREEN - BLACK from left to right.

#### IV. EXPERIMENT

An experimental setup of a vision-based robotic manipulation system has been established in The Chinese University of Hong Kong as shown in Fig. 7, which mainly consists of a 6-DOF robot arm, a camera (Basler acA1920-25gc), a servo robotic gripper, a portable data acquisition module (USB-4751, ADVANTECH), and a computer (operation system: Windows 10). In the first experiment, the separated USB wires were placed beside the soldering groove. The small gripper was controlled to grasp the USB wires in a disorder manner by using vision detection, and then the wire was placed into the corresponding soldering groove. The desired groove position were specified as:  $x_{d1} = [355, 745]^T$  pixel,  $x_{d2} = [455, 746]^T$  pixel,  $x_{d3} = [537, 745]^T$  pixel,  $x_{d4} = [619, 746]^T$  pixel respectively. The position errors are given in Fig. 8, which shows that *Black, Green, Red, White* wires were grasped at  $t \approx 5.73, 12.88, 22.41, 27.86$  s respectively. The total duration of Grasping and Manipulation was around 29 s. The snapshots are shown in Fig. 9.

In the Second experiment, the *Green, White, Red* wire were manually pulled away at  $t \approx 25.6, 56.2$  s after it was manipulated at the desired position, to simulate the scenario that the wire escapes from the groove during the operation of wire pressing. The position errors are shown in Fig. 10 and the snapshots are shown in Fig. 11. At first, the gripper was supposed to grasp then manipulate the *Red* wire after the *Green* wire settled. However, since the *Green* wire was pulled out of the groove, the gripper turned to re-grasping and

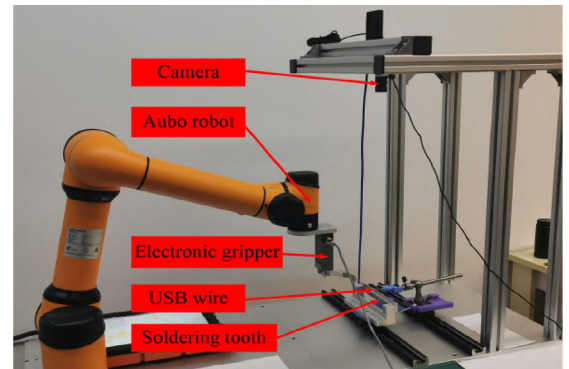


Fig. 7. An experimental setup of a vision-based robotic manipulation system.



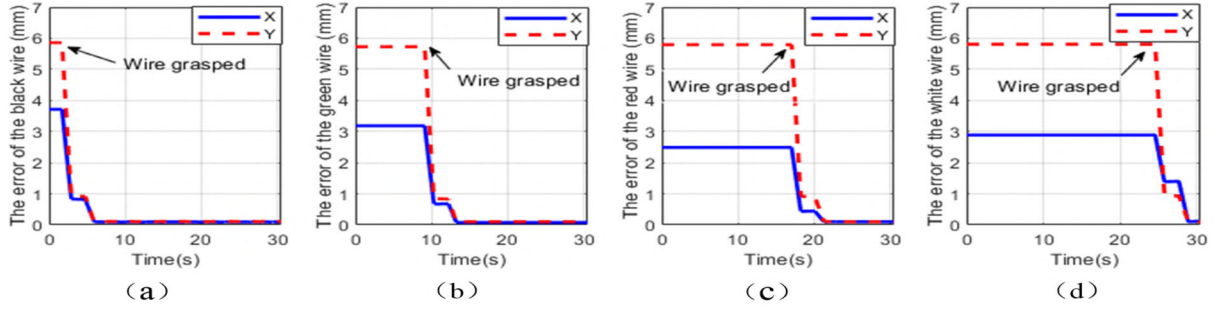


Fig. 8. Experiment 1: the robot performs the grasping and manipulation in a *disorder sequence*. (a) position error for *Black* wire; (b) position error for *Green* wire; (c) position error for *Red* wire; (d) position error for *White* wire;

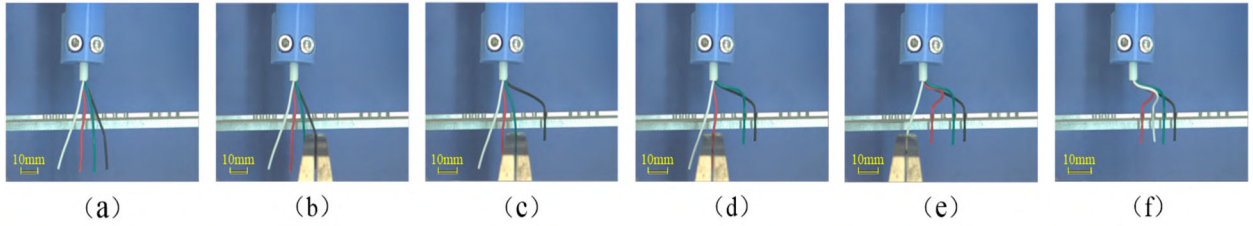


Fig. 9. Snapshots of experiment 1: (a)  $t = 0$  s: initial configuration; (b)  $t = 5.73$  s: grasping and manipulation of the *Black* wire; (c)  $t = 12.88$  s: grasping and manipulation of the *Green* wire; (d)  $t = 22.41$  s: grasping and manipulation of the *Red* wire; (e)  $t = 27.86$  s: grasping and manipulation of the *White* wire. (f)  $t = 31.55$  s: final configuration.

re-manipulating the *Green* wire and then the gripper will still grasp and manipulate the *Red* and *White* wire. After that, the *Red* and *White* are manually pulled away from the soldering groove together. The camera will trigger the compensation control algorithm again, so the *White* and *Red* wire will be re-grasped and re-manipulated to the corresponding groove again. Experimental results show the current control strategy can guarantee the successful grasping and manipulation of the USB wires. In addition, the camera will monitor the status of completion. If the USB wires fall off from the soldering groove, the camera will trigger the compensation control algorithm to re-grasp the corresponding wire. In addition, the developed grasping and manipulating algorithm have the advantage of highly autonomous capability, in sense that no human assistance or supervision is required throughout the procedure.

## V. CONCLUSION

In this paper, a new vision-based grasping and manipulation algorithm has been applied to the sorting and pressing of USB wires. The developed control strategy can sort the disordered USB wires to the desired sequence and it can guarantee the advantage of highly autonomous capability, in the sense that no human assistance or involvement in any steps. Moreover, the sorting sequence is based on the principle of the minimum distance, which means that the USB wires with the smallest distance from the soldering groove has the highest grasping priority. It can also short the

operation time for wire soldering. The experimental results in different scenarios have been presented to demonstrate the performance of the proposed control strategy.

## REFERENCES

- [1] www.cowen.com
- [2] Jose Sanchez, Juan-Antonio Corrales, Belhassen-Chedli Bouzgarrou and Youcef Mezouar, "Robotic Manipulation and Sensing of Deformable Objects in Domestic and Industrial Applications: A Survey," *Int.Journal of Robotics Research*, vol. 18, pp. 3-11, 2018.
- [3] X. Li and C. C. Cheah, "Global task-space adaptive control of robot," *Automatica*, vol. 49, no. 1, pp. 58-69, 2013.
- [4] C. C. Cheah, and X. Li, *Task-Space Sensory Feedback Control of Robot Manipulators*, Springer, 2015.
- [5] J.-J. E. Slotine and L. Weiping, "Adaptive manipulator control: A case study," *IEEE Transactions on Automatic Control*, vol. 33, no. 11, pp. 995-1003, 1988.
- [6] G. Niemeyer and J.-J. E. Slotine, "Performance in adaptive manipulator control," *Int. J. Robot. Res.*, vol. 10, no. 2, pp. 149-161, 1991.
- [7] M. Takegaki and S. Arimoto, "A new feedback method for dynamic control of manipulators," *J. Dyn. Syst., Meas., Control*, vol. 103, no. 2, pp. 119-125, 1981.
- [8] J. R. White, P. E. Satterlee Jr, K. L. Walker, and H. W. Harvey, "Remotely controlled and/or powered mobile robot with cable management arrangement," *U.S. Patent*, 1988.
- [9] V. Mallapragada, N. Sarkar, and T. K. Podder, "Toward a robot-assisted breast intervention system," *IEEE/ASME Trans. on Mechatronics*, vol. 16, no. 6, pp. 1011-1020, 2011.
- [10] D. Navarro-Alarcon, Y.-H. Liu, J. G. Romero, and P. Li, "Model free visually servoed deformation control of elastic objects by robot manipulators," *IEEE Transactions on Robotics*, 26(6):1457-1468, 2013.
- [11] D. Navarro-Alarcon, Y.-H. Liu, J. Romero, and P. Li, "On the visual deformation servoing of compliant objects: Uncalibrated control methods and experiments," *Int. J. Robot. Res.*, vol. 33, no. 11, pp. 1462-1480, 2014.

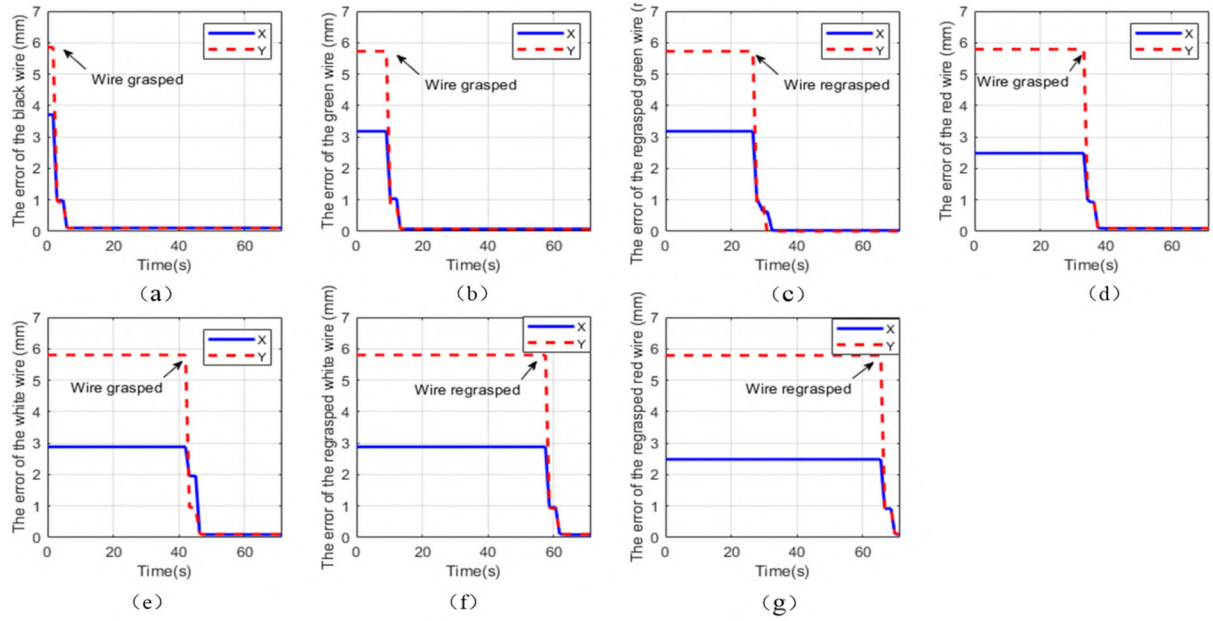


Fig. 10. Experiment 2: The *Green*, *White* and *Red* wire were manually pulled away, and the gripper re-grasped then manipulated it (a) position error for *Black* wire; (b) position error for *Green* wire; (c) position error for re-grasp *Green* wire; (d) position error for *Red* wire; (e) position error for *White* wire; (f) position error for re-grasp *White* wire; (g) position error for re-grasp *Red* wire;

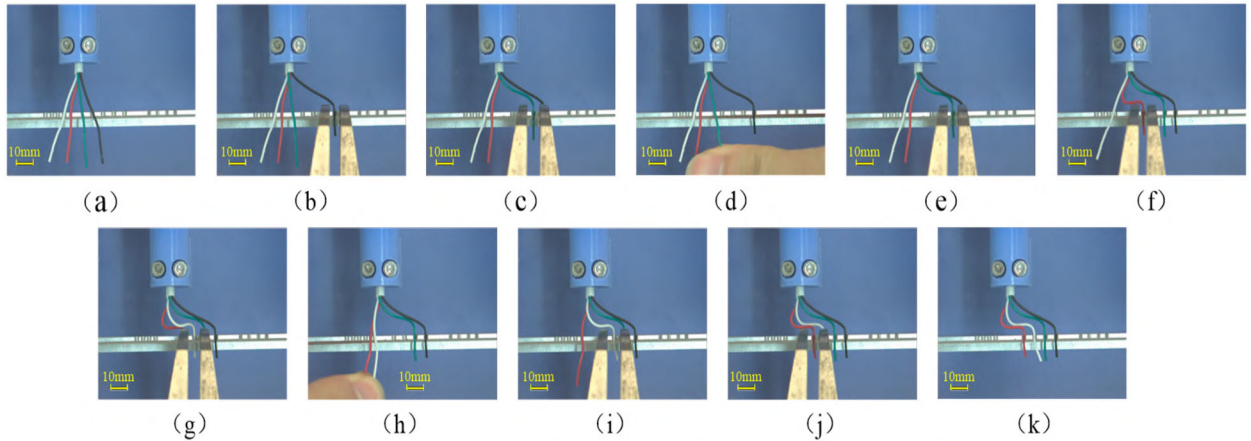


Fig. 11. Snapshots of experiment 2: (a)  $t = 0$  s: initial configuration; (b)  $t = 5.83$  s: grasping and manipulation of the *Black* wire; (c)  $t = 13.21$  s: grasping and manipulation of the *Green* wire; (d)  $t = 25.6$  s: *Green* wire is manually pulled away from the groove; (e)  $t = 30.95$  s: the robot arm re-grasps then re-manipulates the *Green* wire. (f)  $t = 37.6$  s: grasping and manipulation of the *Red* wire; (g)  $t = 46.35$  s: grasping and manipulation of the *White* wire; (h)  $t = 56.2$  s: the *White* and *Red* wires are manually pulled away from the groove together; (i)  $t = 61.85$  s: the robot arm re-grasps the *White* wire; (j)  $t = 69.85$  s: the robot arm re-grasps the *Red* wire; (k)  $t = 71.48$  s: final configuration.

- [12] D. Navarro-Alarcon, H. Yip, Z. Wang, Y.-H. Liu, F. Zhong, T. Zhang, and P. Li, "Automatic 3D manipulation of soft objects by robotic arms with adaptive deformation model," *IEEE Transactions on Robotics*, vol. 32, no. 2, pp. 429-441, 2016.
- [13] Jihong Zhu, Benjamin Navarro, Philippe Fraisse, Andre Crosnier and Andrea Cherubini, "Dual-arm robotic manipulation of flexible cables," *IEEE/RSJ International Conference on Intelligent Robots and Systems*, 2018.
- [14] D. Navarro-Alarcon and Y.-H. Liu, "Fourier-based shape servoing: A new feedback method to actively deform soft objects into desired 2-D image contours," *IEEE Transactions on Robotics*, vol. 34, no. 1, pp. 272-279, 2018.
- [15] Tang, Te and Wang, Changhao and Tomizuka, Masayoshi, "A Framework for Manipulating Deformable Linear Objects by Coherent Point Drift," *IEEE Robotics and Automation Letter*, vol. 3, no. 4, 2018.
- [16] M. Saha and P. Istó, "Manipulation planning for deformable linear objects," *IEEE Transactions on Robotics*, 23(6):1141-1150, 2007.
- [17] M. Moll and L. E. Kavraki, "Path planning for deformable linear objects," *IEEE Transactions on Robotics*, 22(4):625-636, 2006.
- [18] X. Li, Z. Chen, Y. Gao, and Y. Liu, "Apparatus for Separating USB Wires," *U.S. Provisional Patent Application*, no.62/756, 2018.